

# MOSFET-Like Carbon Nanotube Field Effect Transistor Model

Mohammad Taghi Ahmadi, Yau Wei Heong, Ismail Saad, Razali Ismail

Faculty of Electrical Engineering Universiti Teknologi Malaysia  
81310 Skudai, Johor, Malaysia, ahmadiph@gmail.com

## ABSTRACT

An analytical model that captures the essence of physical processes in a CNTFET's is presented. The model covers seamlessly the whole range of transport from drift-diffusion to ballistic. It has been clarified that the intrinsic speed of CNT's is governed by the transit time of electrons. Although the transit time is more dependent on the saturation velocity than on the weak-field mobility, the feature of high-electron mobility is beneficial in the sense that the drift velocity is maintained always closer to the saturation velocity, at least on the drain end of the transistor where electric field is necessarily high and controls the saturation current. The results obtained are applied to the modeling of the current-voltage characteristic of a carbon nanotube field effect transistor. The channel-length modulation is shown to arise from drain velocity becoming closer to the ultimate saturation velocity as the drain voltage is increased.

## 1 INTRODUCTION

There is an intensive search and research for high-speed devices is an ongoing process. Two important factors that determine the speed of a signal propagating through a conducting channel. One is the transit-time or gate delay that depends on the length of the channel and the other is the wire delay that is due to finite RC time constants. The two factors are intertwined as in each one the ultimate saturation of velocity plays a predominant role. The higher mobility brings an electron closer to saturation as high electric field is encountered, saturation velocity remaining the same [Mohammad]. The reduction in conducting channel length of the device results in reduced transit-time-delay and hence enhanced operational frequency. There is no clear consensus on the interdependence of saturation velocity on low-field mobility that is scattering-limited. In any solid state device, it is very clear that the band structure parameters, doping profiles (degenerate or nondegenerate), and ambient temperatures play a variety of roles in determining performance behavior. The outcome that the higher mobility leads to higher saturation is not supported by experimental observations [1, 2]. This paper focuses on the process controlling the ultimate saturation. It has been confirmed in a number of works that the low-field mobility is a function of quantum confinement [3, 4]. In the following, the fundamental processes that limit drift velocity are delineated.

As devices are being scaled down in all dimensions, the

curiosity towards ballistic nature of the carriers is elevated. Initially, it was in the work of Arora[1] that the possibility of ballistic nature of the transport in a very high electric field for a nondegenerate semiconductor was indicated. In this article, the work of Arora is extended to embrace degenerate domain in the carbon nanotube where electrons have analog type classical spectrum only in one direction while the other two directions are quantum confined or digital in nature. When only the lowest digitized quantum state is occupied (quantum limit), a carbon nanotube shows distinct one-dimensional character.

## 2 DISTRIBUTION FUNCTION

In one dimensional nanotube with diameter around nanometer (see Figure. 1), only one of the three Cartesian directions is much larger than the De - Broglie wavelength (Taken is x direction). Since the current is independent of band structure a MOSFET-like CNTFET in the quantum limit can be described by the same theory for semiconductor nanowires MOSFETs. For the Carbon nanotube near the  $k = 0$  band structure is parabolic and the energy spectrum is analog-type only in x-direction.

$$E \approx \frac{E_G}{2} + \frac{\hbar^2 k_x^2}{2m^*} \quad (1)$$

with

$$E_G \approx \frac{2a_{c-c}t}{d} \times \left( \frac{6i - 3 - (-1)^i}{4} \right) \quad i = 1, 2, 3, \dots \quad (2)$$

Here  $E_G$  is the band gap for  $i$ th sub bands and  $a_{c-c}$  is the Carbon -Carbon band in the quantum limit of a nanotube and  $d$  is the diameter of the Carbon nanotube, and  $t=2.7$  (eV) is the nearest neighbor C-C tight binding overlap energy [5, 6]. In the y, z-direction where the length  $L_{y,z} \ll \lambda_D$ , the De - Broglie wavelength  $\lambda_D$  with a typical value of 10 nm.  $k_x$  is the momentum wave vector in the x-direction.  $m^* = 0.05 m_o$  [7].

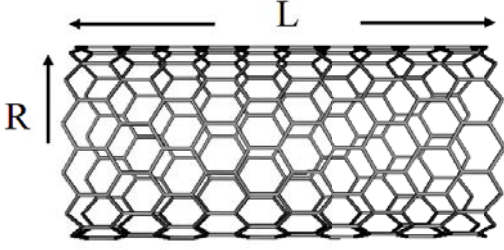


Figure 1. A prototype CNT's (9, 2) with  $R \ll \lambda_D$  and  $L \gg \lambda_D$ .

The quantum wave in the x-direction is a traveling wave and that in the y (z) - direction is the standing wave.

$$\psi_k(x, y, z) = \sqrt{\frac{2}{\Omega}} e^{j(k_x x)} \sin\left(\frac{\pi y}{L_y}\right) \sin\left(\frac{\pi z}{L_z}\right) \quad (3)$$

In carbon nanotube near the minimum band energy similar to one dimensional nanowire we obtain following equation for density of state (DOS).

$$DOS = \frac{\Delta n_x}{\Delta E L_x} = \frac{1}{2\pi} \left(E - \frac{E_G}{2}\right)^{\frac{1}{2}} \left(\frac{2m^*}{\hbar^2}\right)^{\frac{1}{2}} \quad (4)$$

The distribution function of the energy E is given by the Fermi-Dirac distribution function

$$f(E_k) = \frac{1}{e^{\frac{E_k - E_F}{k_B T}} + 1} \quad (5)$$

where  $E_F$  is the one-dimensional Fermi energy at which the probability of occupation is half and T is the ambient temperature. In non-degenerately doped semiconductors the '1' in the denominator of Eq. (5) is neglected as compared to the large exponential factor. In this approximation, the distribution is Maxwellian, which is used in determining the transport parameters extensively. This simplification is good for a nondegenerately-doped semiconductor. However, most nanoelectronic devices these days are degenerately doped. Hence any design based on the Maxwellian distribution is not strictly correct and often leads to errors in our interpretation of the experimental data. In the other extreme, for strongly degenerate carriers, the probability of occupation is 1 when  $E_k < E_F$  and is zero if  $E_k > E_F$ . Arora modified the equilibrium distribution function of Eq. (4) by replacing  $E_F$  (the chemical potential) with the electrochemical potential  $E_F + q\vec{E} \cdot \vec{\ell}$  where  $\vec{E}$  is the applied electric field, q the electronic charge and  $\vec{\ell}$  the mean free path. Arora's distribution function is given by

$$f(E_k) = \frac{1}{e^{\frac{E_k - E_F + q\vec{E} \cdot \vec{\ell}}{k_B T}} + 1} \quad (6)$$

This distribution has a simple interpretation [8, 9] as given in the tilted band diagram. In an extremely large electric field, virtually all the electrons are traveling in the positive x-direction (opposite to the electric field). This is what is meant by conversion of otherwise completely random motion into a streamlined one with ultimate velocity per electron equal to the intrinsic velocity  $v_i$ . Hence the ultimate velocity is ballistic independent of scattering interactions. The ballistic motion in a mean-free path is interrupted by the onset of a quantum emission of energy  $\hbar\omega_0$ . This quantum may be an optical phonon or a photon or any digital energy difference between the quantized energy levels with or without external stimulation present. The mean-free path with the emission of a quantum of energy is related to  $\ell_0$  (zero-field mean free path) by an expression.

$$\ell = \ell_0 \left[1 - e^{-\frac{E_Q}{q\mathcal{E}\ell_0}}\right] = \ell_0 \left[1 - e^{-\frac{\ell_Q}{\ell_0}}\right] \quad (7)$$

$$q\mathcal{E}\ell_Q = E_Q = (N_0 + 1)\hbar\omega_0 \quad (8)$$

$$N_0 = \frac{1}{e^{\frac{\hbar\omega_0}{k_B T}} - 1} \quad (9)$$

Here  $(N_0 + 1)$  gives the probability of a quantum emission.  $N_0$  is the Bose-Einstein distribution function determining the probability of quantum emission. The degraded mean free path  $\ell$  is now smaller than the low-field mean free path  $\ell_0$ .  $\ell \approx \ell_0$  in the Ohmic low-field regime as expected. In the high electric field  $\ell \approx \ell_Q = E_Q / q\mathcal{E}$ . The inelastic scattering length during which a quantum is emitted is given by  $\ell_Q$ . Obviously  $\ell_Q = \infty$  in zero electric field and will not modify the traditional scattering described by mean free path  $\ell_0$  as  $\ell_Q \gg \ell_0$ . The low-field mobility and associated drift motion is therefore scattering-limited. The effect of all possible scattering interactions is now buried in the mean free path  $\ell_0$ . This by itself may be enough to explain the degradation of mobility  $\mu$  in a high electric field; [10]

$$\mu = \frac{q\tau_c}{m^*} = \frac{q\ell}{m^* v_i} \approx \frac{q\ell_Q}{m^* v_i} \quad (10)$$

Here  $\tau_c$  is the mean free time (collision time) during which the electron motion is ballistic.  $v_i$  is the mean intrinsic velocity for 1D carbon nanotube that is discussed in the next section.

### 3 INTRINSIC VELOCITY

The intrinsic velocity is given by

$$v_i = v_{th} \frac{1}{\sqrt{\pi}} \frac{\mathfrak{Z}_0(\eta_F)}{\mathfrak{Z}_{\frac{1}{2}}(\eta_F)} \quad (11)$$

With

$$v_{th} = \sqrt{\frac{2k_B T}{m^*}}, \quad \eta_F = \frac{E_F - \frac{E_G}{2}}{k_B T} \quad (12)$$

$$\mathfrak{Z}_j(\eta) = \frac{1}{\Gamma(j+1)} \int_0^\infty \frac{x^j}{e^{(x-\eta)} + 1} dx \quad (13)$$

Here,  $\mathfrak{Z}_j(\eta)$  is the Fermi-Dirac (FD) integral of order  $j$  and  $\Gamma(j+1)$  is a Gamma function. Its value for an integer  $j$  is  $\Gamma(j+1) = j\Gamma(j) = j!$ . For half integer values, it is  $\Gamma\left(\frac{3}{2}\right) = \frac{1}{2}\Gamma\left(\frac{1}{2}\right) = \frac{1}{2}\sqrt{\pi}$ . In the strongly degenerate regime, the FD integral transforms to

$$\mathfrak{Z}_j(\eta) \approx \frac{1}{\Gamma(j+1)} \frac{\eta^{j+1}}{j+1} = \frac{\eta^{j+1}}{\Gamma(j+2)} \quad (14)$$

The carrier concentration per unit length  $n_1$  is given by

$$n = N_c \mathfrak{Z}_{\frac{1}{2}}(\eta_F) \quad (15)$$

For quasi-one-dimensional carbon nanotubes (CNT) or nanowires, the ultimate average velocity per electron is a function of temperature and doping concentration

$$v_i = \sqrt{\frac{2k_B T}{\pi m^*}} \times \frac{N_c}{n} \mathfrak{Z}_0(\eta_F) \quad (16)$$

With

$$N_c = \left( \frac{2m^* k_B T}{\pi \hbar^2} \right)^{\frac{1}{2}} \quad (17)$$

where  $N_c$  is the effective density of states for the conduction band with  $m^*$  now being the density-of-states effective mass.  $n_1$  is the carrier concentration per unit length. Figure 2 indicates the ultimate velocity as a function of temperature for (9,2) CNT with effective mass  $m^* = 0.099m_0$ . Also shown is the graph for nondegenerate approximation. The velocity for low carrier concentration follows  $T^{1/2}$  behavior independent of carrier concentration. However for high concentration (degenerate carriers) the velocity depends strongly on concentration and becomes independent of the temperature. The ultimate saturation velocity is thus the thermal velocity appropriate for 1D carrier motion:

$$v_{iND} = v_{thd} = \frac{1}{\sqrt{\pi}} v_{th} = \sqrt{\frac{2k_B T}{\pi m_d^*}} \quad (18)$$

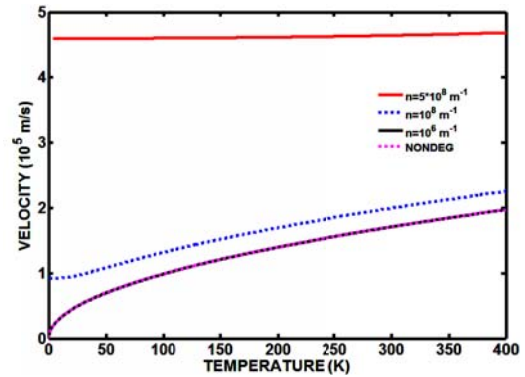


Figure 2. Velocity versus temperature for carbon nanotube for various concentrations.

Figure 3 shows the graph of ultimate intrinsic velocity as a function of carrier concentration for three temperatures ( $T = 4.2$  K,  $77$  K, and  $300$  K). As expected, at a low temperature, carriers follow the degenerate statistics and hence their velocity is limited by an appropriate average of the Fermi velocity that is a function of carrier concentration. When degenerate expression for the Fermi energy as a function of carrier concentration is utilized, the ultimate saturation velocity is given by

$$v_{iD} = \frac{\hbar}{4m^*} (n \pi) \quad (\text{Degenerate}) \quad (19)$$

The ultimate velocity in a quasi-one-dimensional carbon nanotube (CNT) or nanowire may become lower when quantum emission is considered. The inclusion of the quantum or optical phonon or any other similar emission will change the temperature dependence of the saturation velocity.

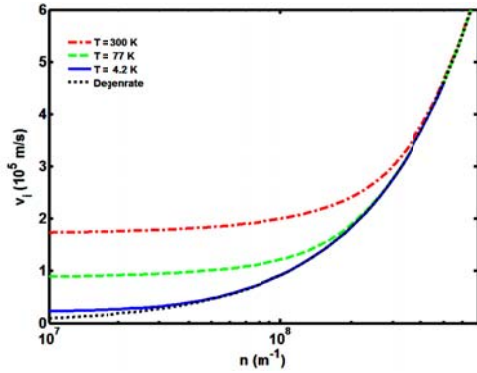


Figure 3 Velocity versus doping concentration for T=4.2 K (liquid helium), T = 77K (liquid nitrogen) and T=300 K (room temperature). In (9,2) semiconducting CNT.

High mobility does not influence the saturation velocity of the carriers, although it may accelerate the approach towards saturation as high fields are encountered in nano-length channels.

#### 4 CARBON NANOTUBE FIELD EFFECT TRANSISTOR

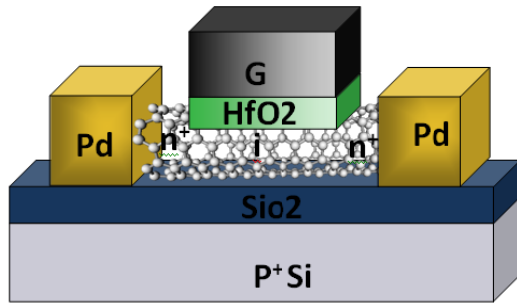


Figure 4 The schematic of a carbon nanotube transistor with gate dielectric.

The velocity saturation effect can conveniently be implemented in the modeling of a carbon nanotube transistor if the empirical relation given below is used.

$$v_D = \frac{\mu_0 E}{E + \frac{E_c}{1 + \frac{E_c}{E}}} \quad (20)$$

With Eq. (20) the drain current  $I_D$  as a function of the gate voltage  $V_{GS}$  and drain voltage  $V_D$  is obtained as

$$I_D = \beta \frac{[2V_{GT}V_D - V_D^2]}{1 + \frac{V_D}{V_c}} \quad (21)$$

with

$$\beta = \frac{\mu_{tf} C_G}{2L} \quad (22)$$

$$V_{GT} = V_{GS} - V_T \quad (23)$$

$$V_c = \frac{v_{sat}}{\mu_{tf}} L \quad (24)$$

where  $C_G$  is the gate capacitance per unit length, and  $L$  the effective channel length.  $V_T$  is the threshold voltage. The value of  $\mu_{tf} = 60000 \text{ cm}^2/\text{V.s}$  is taken.  $v_{sat} = v_{il}$  is the intrinsic velocity of Eq. (19). In the absence of quantum emission for (9, 2) semiconductor carbon nanotube the intrinsic carrier concentration is  $n_i = 7.921 \times 10^{13} \text{ m}^{-3}$  [11,12]. Because of the unknown nature of the quantum emission, it is ignored in this calculation. With the simple geometry of the carbon nanotube transistor of Figure 4, the gate capacitance is given by  $C_G = (C_e C_Q) / (C_e C_Q + 1)$ , where  $C_e$  is the electrostatic gate coupling capacitance of the gate oxide and  $C_Q$  is the quantum capacitance of the gated SWCNT. The quantum capacitance  $C_Q$  arises from the fact that the electron wave function vanishes at the carbon nanotube (CNT)-insulator interface [14]. For a carbon nanotube of length,  $L$  and radius,  $r$  capacitance comes out to be [15].

$$C_e \approx \frac{2\pi\epsilon}{\ln \left[ \frac{t_{ox} + r + \sqrt{t_{ox}^2 + 2t_{ox}r}}{r} \right]} L \quad [25]$$

where  $\epsilon$ ,  $t_{ox}$ , and  $r$  are the dielectric constant and thickness of oxide, and the radius of SWCNTs, respectively [16, 17,18]. Using  $\epsilon = 20\epsilon_0$ ,  $t_{ox} = 80 \text{ nm}$ ,  $L = 250 \text{ nm}$  and  $r = 1.7 \text{ nm}$ . which for typical experimental setups is in the order of tens of aF/ $\mu\text{m}$ . To add to this, the quantum capacitance in carbon nanotubes is of considerable significance. The quantum capacitance can be write as [19]  $C_Q = 2e/v_F$  where,  $v_F \approx 10^6 \text{ m/s}$  is the Fermi velocity of electrons in the CNT [20]. Numerically  $C_Q$  comes out to be 76.5 aF/ $\mu\text{m}$  shows thereby that both electrostatic as well

as the quantum capacitances play important role in the CNTs. [21,22]. At the onset of current saturation, all carriers leave the channel at the saturation velocity where electric field is extremely high. Therefore, the saturation current is given by

$$I_{Dsat} = C_G (V_{GT} - V_{Dsat}) v_{sat} \quad (26)$$

When Eqs. (21) and (26) at the onset of current saturation are consolidated, the drain voltage at which the current saturates is given by.

$$V_{Dsat} = V_c \left[ \sqrt{1 + \frac{2V_{GT}}{V_c}} - 1 \right] \quad (27)$$

With this value of  $V_{Dsat}$  substituted in Eq. (26), the saturation current is given by

$$I_{Dsat} = \beta V_{Dsat}^2 \quad (28)$$

Figure 5 shows the current-voltage characteristics of a transistor with  $L = 250$  nm. In this regime,  $V_{GT} > V_c$ . The steps in I-V characteristics tend to be equally spaced as  $V_{GT}$  becomes much larger than  $V_c$ . An analysis of the velocity distribution in the channel indicates that the velocity throughout the length of the channel is lower than that on the drain end where carriers are moving with the maximum permissible velocity. The equally-spaced step behavior of I-V characteristics is in direct contrast to the behavior expected from long channel transistors ( $V_{GT} \ll V_c$ ), when steps separation varies quadratic ally with the adjusted gate voltage  $V_{GT}$ . In fact, if Eqs. (21) is expanded to second order in  $V_{GT}$ , one can easily notice the complete absence of pinch off effect[23].

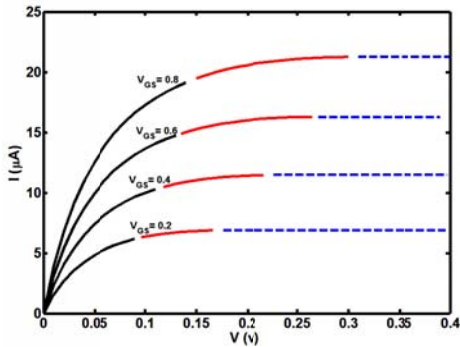


Figure .5. Current -Voltage characteristics of nanowire.

## 5 CONCLUSIONS

Intrinsic speed of carriers in CNT's is governed by the transit time of electrons. Although the transit time is more dependent on the saturation velocity than on the weak-field mobility, the feature of high-electron mobility is beneficial in the sense that the drift velocity is maintained always closer to the saturation velocity, at least on the drain end of the transistor where electric field is necessarily high and controls the saturation current.

In many ways, the distribution function reported is similar to what is presented by Buttiker [24]. A series of ballistic channels of length  $\ell$  comprise a macro-channel of length  $L$ . The behavior is well understandable as we consider ballistic low-field mobility where  $\ell$  is replaced by  $L$ . However, it does not affect the velocity saturation in high electric field that is always ballistic. The ends of each mean free path thus can be considered Buttiker's thermalizing virtual probes, which can be used to describe transport in any regime. In high electric field, the electrons are in a coordinated relay race, each electron passing its velocity to the next electron at each virtual probe. The saturation velocity is thus always ballistic whether or not device length is smaller or larger than the mean free path. The ballistic saturation velocity is always independent of scattering-limited low-field mobility that may be degraded by the gate electric field. The relation between mobility and the mean free path has deep consequences on the understanding of the transport in a nanoscale device.

The importance of developing FET structures with high electron concentrations and high current-drive capabilities is emphasized. The current drive can be enhanced by an array of CNT's transistors particularly for high speed digital applications. The switching speed is usually determined by the charging process of capacitive loads, including interconnects. The presence of a tradeoff relation between high mobility and high doping concentration is required to optimize performance of the CNT's transistor following the recommendations of Sakaki [25]. The channels can be designed for the benefit of utilizing selectively doped double-heterojunctions and other FET nanostructures. The role of the quantum engineering by the gate-field induced mobility degradation in determining low-field electron mobility is indicated. Also, the role of quantum waves in determining the correct capacitance to make quantitative interpretations of the gate capacitance is required. Although the technical difficulty encountered in the preparation of a CNT transistor is far greater than that for 2D nanostructures, there appear to be several bright prospects if one develops novel schemes of microfabrications, including the use of edge of quantum-well nanostructures as the theory guides the experimenters toward the design of CNT transistors and allows them to assess performance accordingly.

## ACKNOWLEDGEMENT

The authors would like to thank Malaysian Ministry of Science, Technology and Industry (MOSTI) for a research grant for support of postgraduate students. The work is supported by UTM Research Management Center (RMC).

## REFERENCES

- [1] V. K. Arora, "High-Field Distribution And Mobility In Semiconductors," Japanese Journal Of Applied Physics ,Jpn. J. Appl. Phys 24, P. 537, 1985.
- [2] Hui Houg Lau, M.Taghi Ahmadi\*, Razali Ismail, ,Vijay K. Arora "Current-Voltage Characteristics Of A Silicon Nanowire Transistor" Proceedings Of The Wra-Ldsd 7-9 April (2008) Nottingham
- [3] Vijay K. Arora, "Quantum Well Wires: Electrical And Optical Properties," J.Phys. C:, Vol.18, Pp. 3011-3016, 1985.
- [4] Vijay K. Arora, Michael L. P. Tan, Ismail Saad, And Razali Ismail, "Ballistic Quantum Transport In A Nanoscale Metal-Oxide-Semiconductor Field Effect Transistor," Applied Physics. Letters, Vol. 91, Pp. 103510-103513, 2007.
- [5] Vijay K. Arora, "Failure Of Ohm's Law: Its Implications On The Design Of Nanoelectronic Devices And Circuits," Proceedings Of The Ieee International Conference On Microelectronics, May 14-17, 2006, Belgrade, Serbia And Montenegro, Pp. 17-24.
- [6] R. A. Jishi, D. Inomata, K. Nakao, M. S. Dresselhaus, And G. Dresselhaus, "Electronic And Lattice Properties Of Carbon Nanotubes," J.Phys.Soc.Jap., Vol. 63, No. 6, Pp. 2252–2260, 1994.
- [7] A. M. T. Fairus And V. K. Arora, "Quantum Engineering Of Nanoelectronic Devices: The Role Of Quantum Confinement On mobility Degradation," Microelectronics Journal, Vol. 32, Pp. 679-686, 2000.
- [8] Mark S. Lundestorm, And, Jing Guo Nanoscale Transistors: Device Physics, Modeling and Simulation. Spriger, New York, 2006.
- [9] V. K. Arora, "Quantum Engineering Of Nanoelectronic Devices: The Role Of Quantum Emission In Limiting Drift Velocity And Diffusion Coefficient," Microelectronics Journal, Vol. 31, No.11-12, Pp 853-859. 2000.
- [10] H. Ishii, N. Kobayashi, K. Hirose, Contact And Phonon Scattering Effects On Quantum Transport Properties Of Carbon-Nanotube Field-Effect Transistors, Applied Surface Science (2007), Doi:10.1016/J.Apsusc.2008.01.116
- [11] Gianluca Fiori, Giuseppe ,Threshold Voltage Dispersion And Impurity Scattering Limited Mobility In Carbon Nanotube Field Effect Transistors With Randomly Doped Reservoirs Iannaccone2006 IEEE
- [12] Jose M. Marulanda, Ashok Srivastava1 Carrier Density and Effective Mass Calculations for Carbon Nanotubes 2007 IEEE
- [13] S. Ilani\*, L. A. K. Donev, M. Kindermann and P. L. Mceuen\* Measurement of the Quantum Capacitance of Interacting Electrons in Carbon Nanotubes Nature Physics Vol 2 October 2006
- [14] Changxin Chen , Zhongyu Hou, Xuan Liu, Eric Siu-Wai Kong, Jiangping Miao, Yafei Zhang Fabrication And Characterization Of The Performance Of Multi-Channel Carbon-Nanotube Field-Effect Transistors 0.1016/J. Physleta. 2007
- [15] Jose M. Maruland, Ashok Srivastavand Siva Yellampalli," Numerical Modeling of the I-V Characteristic of Carbon Nanotube Field Effect Transistors" 40th Southeastern Symposium on System Theory, March 16-18, 2008
- [16] J.Q. Li, Q. Zhang, D.J. Yang, J.Z. Tian, Carbon 42 (2004) 2263.
- [17] A. Javey, H. Kim, M. Brink, Q. Wang, A. Ural, J. Guo, P. McIntyre, P. Mceuen, M. Lundstrom, H. Dai, Nature Mater. 1 (2002) 241.
- [18] R. Martel, T. Schmidt, H.R. Shea, T. Hertel, P. Avouris, Appl. Phys.Lett. 73 (1998) 2447
- [19] P.J. Burke. An Rf Circuit Model For Carbon Nanotubes. Ieee Trans Nanotechnology, 2(1):55–58, March 2003.
- [20] Y.-M. Lin, J. Appenzeller , Z. Chen , Z.-G. Chen, H.-M. Cheng, and Ph. Avouris," Demonstration of a High Performance 40-nm-gate Carbon Nanotube Field-Effect Transistor" 0-7803-9040-2005 IEEE
- [21] Sandeep K. Shukla, R. Iris Bahar," Nano, Quantum And Molecular Computing "Kluwer Academic Publishers, 2004
- [22] J. W. G. Wild"Oer, L. C. Venema, A. G. Rinzler, R. E. Smalley, And C. Dekker, Electronic Structure Of Atomically Resolved Carbon Nanotubes," Nature (London), Vol. 391, No. 6662, Pp. 59–62, 1998.
- [23] H. Sakaki, Scattering Suppression And High-Mobility Effect Of Size Quantized Electrons In Ultrafine Semiconductor Wire Structures," Jpn. J. Appl. Phys., Vol. 19, Pp. L735-L738, 1980.
- [24] M. Buttiker, "Role Of Quantum Coherence In Series Resistors," Phys. Rev. B, Condens. Matter, No. 33, Pp. 3020–3026, 1986.
- [25] H. Sakaki, "Velocity Modulation Transistor (Vmt)- A New Field-Effect transistor concept," Jpn. J. Appl. Phys., Vol. 21, Pp. L381-L383, 1982.